Structure and bonding nature of C_{60}/Si(100)-c(4×4): Density-functional theory calculations

Ji Young Lee and Myung Ho Kang
Department of Physics, Pohang University of Science and Technology, Pohang 790-784, Korea
(Received 13 September 2006; revised manuscript received 10 January 2007; published 6 March 2007)

We have studied the adsorption structure and bonding nature of the C_{60}/Si(100)-c(4×4) surface using density-functional theory calculations. Based on energetics and scanning-tunneling-microscopy simulations, we propose a structural model where C_{60} adsorbs in between Si dimer rows with a C–C bond shared by two hexagon faces headed down and aligned perpendicular to Si dimer rows. This structure shows a semiconducting band structure, and the modified occupied and unoccupied molecular-orbital levels are resolved. Our charge character analysis figures out the bonding nature as covalent by the evidence of C–Si σ bond formations. The calculated surface density of states, well reflecting the modified molecular levels, explains well the position and origin of the peaks measured by photoelectron spectroscopy study.

DOI: 10.1103/PhysRevB.75.125305 PACS number(s): 68.47.Fg, 72.80.Rj, 73.20.At, 68.43.Bc

I. INTRODUCTION

The interface of large organic molecules with solids has attracted much interest in molecular electronics, because the understanding of the interface interaction and bonding mechanism is crucial for designing and controlling desired properties at nanometer scale in the fabrication of electronic devices.[1,2] As a prototype nanomolecule, C_{60} has interesting properties such as a large spherical shape, high symmetry, and ease of handling and is expected to provide useful structural, electronic, and optical functionalities.[3–5] Particularly, C_{60} overlayer structures on the Si(100) surface have received great attention in connection with the development of new molecular devices combined with current semiconductor technology.

C_{60} molecules are known to form local orderings on Si(100) at room temperature (RT). Two local orderings, c(4×4) and c(4×3), have been commonly observed by scanning-tunneling-microscopy (STM) experiments,[6–8] and these are defined as one monolayer (ML) configurations. STM experiments[6–8] reported that, while C_{60} adsorbs at only one site (T) in the c(4×4) ordering, two different sites (T and T') are equally occupied in the c(4×3) ordering. T and T' represent two distinguished trench sites between dimer rows: While T locates at the center of four Si dimers (see Fig. 1), T' locates at the center of two Si dimers. Hashizume *et al.*[7] proposed two possible molecular orientations of C_{60}, one with a C–C bond shared by two hexagon faces (denoted as a HH bond, hereafter) toward the surface, aligned parallel to Si dimer rows, and the other with the same C–C bond aligned perpendicular to Si dimer rows. The bonding nature of C_{60} on Si(100) is still under debate. In experimental studies of 1 ML C_{60}/Si(100), both physisorption[9,10] and chemisorption[6,7,11] have been reported. Photoelectron spectroscopy (PES) studies[12,13] reported coverage-dependent results: The interaction between C_{60} and Si(100) appears as covalent at 0.25 ML, but the interaction gets weaker at 1 ML. In order to understand the structure and bonding nature of C_{60}/Si(100), first-principles calculations for both atomic and electronic structures are desirable. There have been theoretical studies mainly focused on the electronic structure of C_{60} overlayers,[14–17] but none of them correctly took into account the underlying Si(100) substrate structure.

In this paper, we determine the adsorption geometry and electronic structure of the C_{60}/Si(100)-c(4×4) surface using density-functional theory (DFT) calculations. First, we carry out energetics calculations and STM simulations for several structural models and propose the adsorption structure by comparing with STM experiments. Next, we examine the band structure and the charge character of molecular orbitals to clarify the bonding nature between C_{60} and Si(100). Finally, we compare the calculated surface density of states with PES measurement and verify the structural origins of the observed peaks.

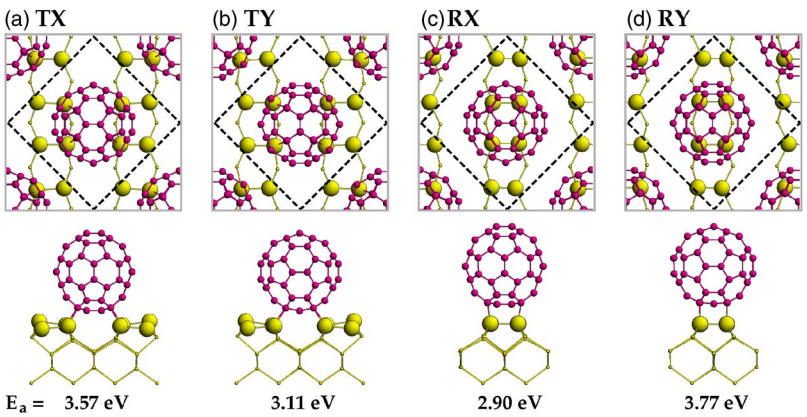

FIG. 1. (Color online) Structural models for C_{60}/Si(100)-c(4×4). Dashed lines represent the c(4×4) surface unit cell and the largest balls Si dimers. The models are named after the adsorption site and the molecular orientation. For example, TX stands for the T site and the X orientation. The structures represent the optimized adsorption geometries, and the adsorption energies (E_a) are given in eV/molecule.

II. METHOD

DFT calculations have been performed using the local-density approximation for exchange and correlation.[18,19] We employ ultrasoft pseudopotentials[20] for C atoms and norm-conserving pseudopotentials[21] for Si and H atoms and use a plane-wave basis with a cutoff energy of 25 Ry. We take 8 **k** points in the c(4×4) surface Brillouin zone for the **k**-space integration. The Si(100) surface is simulated by a repeated slab geometry. Each slab consists of six Si layers, and two adjacent slabs are separated by ten vacuum layers. C_{60} molecules are adsorbed on the top side of the slab with the bottom side passivated by H atoms. All atoms but the bottom two Si layers are relaxed until the force components of each atom are within 0.025 eV/Å. Similar calculation schemes were used in our previous studies on molecule-surface interactions,[22,23] and test calculations have shown that, for two energetically favored C_{60} adsorption models, the adsorption energy difference is converged within 0.05 eV and the C–C and C–Si bond lengths within 0.01 Å with respect to the plane-wave cutoff energy, the number of **k** points, and the supercell size. We simulate STM images of the optimized structures by constant-density topographs of the surface electronic charge, which is obtained by integrating the local density of states $\rho(r,E)$ between the Fermi level and a chosen bias voltage.

III. RESULTS

We consider four structural models for the C_{60}/Si(100)-c(4×4) surface (see Fig. 1). In the first two models (TX and TY), C_{60} molecules occupy the same *T* site but with different molecular orientations, *X* and *Y*, respectively. *X* (*Y*) represents that the direction of the bottom HH bond is perpendicular (parallel) to Si dimer rows. The other models, RX and RY, represent the structures with C_{60} adsorbed on the dimer rows along the *X* and *Y* molecular directions, respectively. TX and TY were proposed as the structural models for C_{60}/Si(100)-c(4×4) in a previous STM experiment,[7] and RX and RY were considered as models for the 0.5 ML p(4×4) structure in a recent DFT study.[24]

We optimize the four models and calculate the adsorption energies, defined as the energy gain per C_{60} molecule relative to the free C_{60} molecule and the clean Si(100)-(2×2) buckled surface. In energetics, the RY structure is found to be the most stable with the adsorption energy of 3.77 eV. The bond lengths of four C–Si bonds are 1.95–1.96 Å. Although the other structures have similar C–Si bond lengths of 1.97–2.00 Å, their adsorption energies are at variance: While the RX and TY structures are far less stable than the RY structure, the TX structure appears relatively stable with a small energy difference of 0.20 eV.

Figure 2 shows the simulated filled-state STM images for the four structural models. The simulations at a bias of −1.5 eV are found to simply reproduce the highest occupied molecular-orbital (HOMO) images of a free C_{60} molecule. The images obtained at a bias of −0.6 eV appear different from the simple HOMO images, reflecting the effect of the molecular interactions with the Si(100) substrate: The most

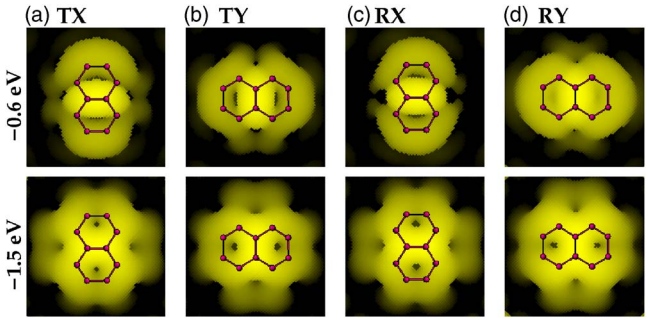

FIG. 2. (Color online) Simulated constant-current filled-state STM images of the four adsorption models considered for C_{60}/Si(100)-c(4×4). The images were obtained by integrating the local density of states $\rho(r,E)$ from E_F to the bias voltages. The images of −1.5 and −0.6 eV were taken at $\rho=6.7\times10^{-4}$ and 6.7×10^{-5} e/Å^3, respectively. Two top hexagon faces of the adsorbed C_{60} molecule are shown.

stable RY structure shows a bright image of oval shape representing the top HH bond of C_{60} and two surrounding less bright images. The other structures show similar images to that of the RY structure but with clearly distinguished orientations corresponding to their *X* or *Y* molecular orientation. In their STM study, Hashizume *et al.*[7] proposed the TY model as the underlying structure for the observed filled-state C_{60} images of three or four stripes aligned perpendicular to Si dimer rows. Their assignment of the *Y* molecular orientation was based on a comparison with the calculated charge distribution of the c(4×3) array of C_{60} reported in a DFT study of Kawazoe *et al.*[25] In a later DFT study of the C_{60}/Si(100)-c(4×4) surface, Yajima and Tsukada[16] found that the TY structure reproduces well the STM images of Hashizume *et al.*[7] The accuracy of the previous DFT studies, however, is in question because the Si(100) substrate was not properly taken into account: Kawazoe *et al.*[25] focused on the two-dimensional array of C_{60} and treated the Si(100) substrate as too simplified a positive charge background. Yajima and Tsukada[16] assumed the interface C–Si bond lengths to be the sum of the atomic radii and neglected the atomic relaxation. It is clearly shown in the present STM simulations, by taking correctly into account the interaction between C_{60} and Si(100), that the experimental image of stripes perpendicular to Si dimer rows is reproduced by the *X* molecular orientation, not by the *Y* orientation. Of the two models with the *X* molecular orientation, the TX structure is much more stable by 0.67 eV than the RX structure in agreement with the *T*-site proposal for c(4×4) by STM experiments.[6–8] We thus propose the TX structure as the model for the observed c(4×4) ordering.[6–8]

It is interesting why the experimental c(4×4) structure is not the most stable RY structure but a less stable TX structure. We note that the experimental c(4×4) ordering was formed at RT without annealing.[6–8] It is known in STM experiments[6–8,26–28] that, at RT, C_{60} molecules reside at the *T* site at low coverages. The DFT study of Hobbs *et al.*[24] also demonstrated that the TX structure is the most energetically favorable structure for the 0.5 ML p(4×4) configuration. We thus speculate that, in the 1 ML c(4×4) phase, the most

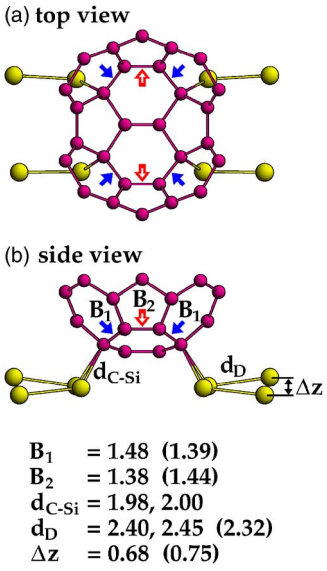

FIG. 3. (Color online) Adsorption geometry of the TX structure for C_{60}/Si(100)-c(4×4). For clarity, only the lower part of the adsorbed C_{60} molecule and Si dimers are shown. The bond lengths are given in Å ($d_{C\text{-}Si}$ and d_D have two distinct values due to the dimer bucklings). The numbers in parentheses represent the reference values for the free C_{60} and the Si(100)-(2×2) buckled surface.

stable RY structure is kinetically inaccessible: Once C_{60} molecules preferentially occupy *T* sites at low coverages, later R-site adsorptions would be hindered by the repulsion from the preadsorbed C_{60} molecules. For example, in the p(4×4) configuration, while an additional *T*-site adsorption leads to a nearest-neighbor molecular separation of 10.9 Å,[6–8] an additional *R*-site adsorption results in a molecular separation of 8.6 Å, significantly smaller than the van der Waals separation (10.0 Å) in the fcc C_{60} solid.[29,30] Therefore, once the TX structure is initialized at low coverages, additional C_{60} adsorptions would maintain the TX configuration, leading to the 1 ML c(4×4) ordering with the TX structure.

Figure 3 shows the details of the TX adsorption geometry. Noticeable are the changes in the C–C bonding configuration due to the interaction with Si(100): Four short bonds (denoted as B_1) are elongated by 0.09 Å from 1.39 Å, while two long bonds (B_2) are contracted by 0.06 Å. Similar C–C rebonding configurations are also found in the TY, RX, and RY structures: their B_1 and B_2 bond lengths agree within 0.01 Å to those of the TX structure. (B_1 and B_2 are defined as the same because the C atoms bonded to Si atoms are the same in all models.) These structural changes indicate that the π bondings of the four short bonds (B_1) are broken and participate in forming two new C–C π bonds (B_2) and additional bondings with Si atoms. We note that similar formation of two new C–C π bonds was reported in previous calculations for the 0.5 ML p(4×4) phase.[24,31] The bonding between C_{60} and Si(100) is characterized by four C–Si bonds. The calculated C–Si bond lengths (1.98 and 2.00 Å) are close to 1.94 Å, the sum of the atomic radii of C and Si in diamond structure, implying a covalent character of the C–Si bonding. The bonding nature is clarified shortly in the electronic structure analysis. The structure of the Si dimers is also affected. The buckling is still maintained, but the magnitude decreases from 0.75 Å of the clean surface to 0.68 Å, and the dimer bond lengths increase from 2.32 Å to 2.40 and 2.45 Å.

The C_{60}/Si(100)-c(4×4) TX structure shows a semiconducting band structure as shown in Fig. 4. The interaction with Si(100) splits the degenerate HOMO states of the free C_{60} molecule into the states labeled as H_1, H_2, and H_3, which were found to maintain the charge character of C–C π bondings. While the H_2 states remain similar in energy to the HOMO level, the H_1 and H_3 states are shifted by about ±0.5 eV. These affected states reflect well the interfacial C–Si interactions. Figure 4(b) displays the charge distributions of two representative H_1 and H_3 states, which clearly represent the character of C–Si σ bonding states. The C–Si covalent bonding is responsible for the split of the C_{60} HOMO states on Si(100). In the empty states, the lowest unoccupied molecular-orbital (LUMO) and the next-level (LUMO+1) states of the free C_{60} also split and form states with the charge character of the C–C π^* antibondings, denoted as L_1 and L_2, respectively. The LUMO+1 level undergoes a large change by the C–Si interaction, leaving no trace at the original molecular level. Dangling bonds of the intact Si dimer atoms form four bands near the Fermi level (represented by dots) in between the H_1 and L_1 levels: two filled

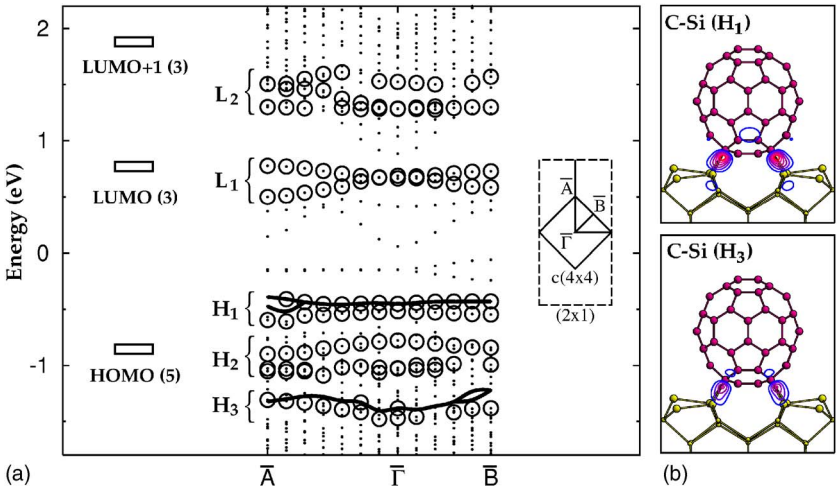

FIG. 4. (Color online) (a) Band structure of the TX structure for C_{60}/Si(100)-c(4×4). Empty circles represent the molecular states containing more than 50% of charge in C_{60} molecule. For comparison, the molecular levels of a free C_{60} are shown on the left side. Solid lines represent the states participating in C–Si σ bondings. All energies are given relative to the Fermi level. (b) The charge characters of the C–Si σ bonding states at $\bar{\Gamma}$ point. In the contour plot, a uniform increment of 6.5×10^{-3} e/Å^3 is used.

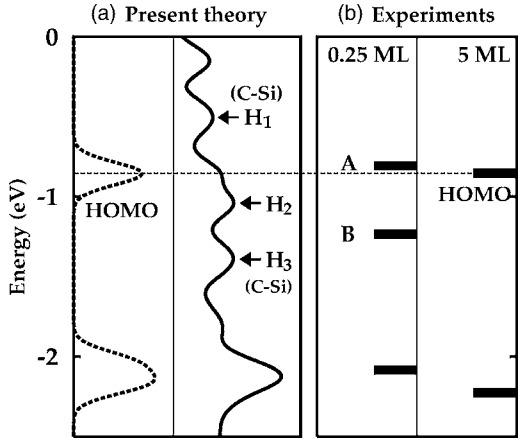

FIG. 5. (a) Surface density of states (SDOS) of the C_{60}/Si(100)-c(4×4) TX structure obtained by integrating the local density of states over the surface region including the outermost two Si layers and C_{60} molecule. The density of states of a free C_{60} is shown as dashed lines for comparison. (b) Peak positions in PES (Refs. 12 and 13) spectra. The PES data are aligned to match the HOMO level measured at 5 ML to the calculated HOMO level of a free C_{60}.

bands for the two up-dimer Si atoms and two empty bands for the two down-dimer Si atoms.

Figure 5(a) shows the calculated surface density of states (SDOS) for the C_{60}/Si(100)-c(4×4) TX structure. The HOMO-derived H_1-H_3 levels mentioned in the band structure appear as prominent peaks in SDOS, which can be compared with previous experiments. In their PES study, Suto *et al.*[12] and Sakamoto *et al.*[13] observed that the HOMO level measured at 5 ML splits into two peaks at 0.25 ML [denoted as A and B in Fig. 5(b)]. Here, the 5 ML film was reported to have the same spectral feature as that of a bulk C_{60},[9,12] and this spectral feature is in good accord with our calculation for the free C_{60}. The peaks A and B observed at 0.25 ML were assigned to shifted HOMO levels and C–Si bonding states, respectively.[12,13] We find that the PES peaks A and B compared well in peak position with the calculated peaks H_2 and H_3, respectively. Our finding that the peak H_3 contains C–Si bonding states also supports the experimental assignment of the peak B to C–Si bonding states.

In PES studies,[10,13] 1 ML C_{60} samples prepared at RT were found to show the same spectral profile as that of the 5 ML film, leading to the suggestion that most of C_{60} molecules in the 1 ML samples are physisorbed on Si(100). This suggestion is in line with the STM observations[6–8] that 1 ML samples prepared at RT are rather disordered and have two partially ordered configurations, c(4×3) and c(4×4). Therefore, the present SDOS calculations for the 1 ML c(4×4) ordered phase, where all the C_{60} molecules reside in the TX configuration, could not be fairly compared with the 1 ML experimental results. On the other hand, at coverages as low as 0.25 ML, C_{60} molecules prefer the TX structure, as was addressed before.[6–8,24,26–28] It is thus natural that the experimental features at 0.25 ML compared well with the present c(4×4) calculations based on the same local geometry, the TX structure.

IV. CONCLUSION

In summary, we have investigated the C_{60}/Si(100)-c(4×4) surface using DFT calculations. We found that covalent bondings are formed between C_{60} and Si(100). We proposed the TX structure as the adsorption model for the experimental samples. This structure is in accord with STM measurements and also explains well the positions and origins of the peaks observed in PES experiment. The TX structure, however, is not the most stable configuration. The most stable configuration, the RY structure, may not be kinetically accessible at RT. It is of great interest that this thermodynamic ground state would be realized by annealing.

ACKNOWLEDGMENTS

This work was supported by the Korea Research Foundation Grant funded by the Korean Government (KRF-2005-041-C00129). Computations were performed using the supercomputing facilities at POSTECH and KISTI.

[1] M. A. Reed, C. Zhou, C. J. Muller, T. P. Burgin, and J. M. Tour, Science **278**, 252 (1997).
[2] J. Schnadt, P. A. Brühwiler, L. Patthey, J. N. O'Shea, S. Södergren, M. Odelius, R. Ahuja, O. Karis, M. Bässler, P. Persson, H. Siegbahn, S. Lunell, and N. Mårtensson, Nature (London) **418**, 620 (2002).
[3] H. Park, J. Park, A. K. L. Lim, E. H. Anderson, A. P. Alivisatos, and P. L. McEuen, Nature (London) **407**, 57 (2000).
[4] C. Joachim, J. K. Gimzewski, and A. Aviram, Nature (London) **408**, 541 (2000).
[5] J. A. Theobald, N. S. Oxtoby, M. A. Phillips, N. R. Champness, and P. H. Beton, Nature (London) **424**, 1029 (2003).
[6] X.-D. Wang, T. Hashizume, H. Shinohara, Y. Saito, Y. Nishina, and T. Sakurai, Phys. Rev. B **47**, 15923 (1993).
[7] T. Hashizume and T. Sakurai, J. Vac. Sci. Technol. B **12**, 1992 (1994).
[8] A. W. Dunn, E. D. Svensson, and C. Dekker, Surf. Sci. **498**, 237 (2002).
[9] S. Suto, K. Sakamoto, T. Wakita, C.-W. Hu, and A. Kasuya, Phys. Rev. B **56**, 7439 (1997).
[10] K. Sakamoto, D. Kondo, Y. Ushimi, M. Harada, A. Kimura, A. Kakizaki, and S. Suto, Phys. Rev. B **60**, 2579 (1999).
[11] C.-P. Cheng, T.-W. Pi, C.-P. Ouyang, and J.-F. Wen, J. Vac. Sci. Technol. B **23**, 1018 (2005).
[12] S. Suto, K. Sakamoto, D. Kondo, T. Wakita, A. Kimura, and A. Kakizaki, Surf. Sci. **427**, 85 (1999).
[13] K. Sakamoto, D. Kondo, M. Harada, A. Kimura, A. Kakizaki, and S. Suto, Surf. Sci. **433**, 642 (1999).
[14] T. Yamaguchi, J. Vac. Sci. Technol. B **12**, 1932 (1994).
[15] A. Yajima and M. Tsukada, Surf. Sci. **357**, 355 (1996).

[16] A. Yajima and M. Tsukada, Surf. Sci. **366**, L715 (1996).
[17] G.-C. Liang and A. W. Ghosh, Phys. Rev. Lett. **95**, 076403 (2005).
[18] D. M. Ceperley and B. J. Alder, Phys. Rev. Lett. **45**, 566 (1980).
[19] J. P. Perdew and A. Zunger, Phys. Rev. B **23**, 5048 (1981).
[20] D. Vanderbilt, Phys. Rev. B **41**, 7892 (1990).
[21] N. Troullier and J. L. Martins, Phys. Rev. B **43**, 1993 (1991).
[22] S. H. Lee and M. H. Kang, Phys. Rev. B **58**, 4903 (1998).
[23] J. Y. Lee and M. H. Kang, Phys. Rev. B **69**, 113307 (2004).
[24] C. Hobbs, L. Kantorovich, and J. D. Gale, Surf. Sci. **591**, 45 (2005).
[25] Y. Kawazoe, H. Kamiyama, Y. Maruyama, and K. Ohno, Jpn. J. Appl. Phys., Part 1 **32**, 1433 (1993).
[26] D. Chen and D. Sarid, Surf. Sci. **329**, 206 (1995).
[27] X. Yao, T. G. Ruskell, R. K. Workman, D. Sarid, and D. Chen, Surf. Sci. **367**, L85 (1996).
[28] P. Moriarty, Y. R. Ma, M. D. Upward, and P. H. Beton, Surf. Sci. **407**, 27 (1998).
[29] W. Krätschmer, L. D. Lamb, K. Fostiropoulos, and D. R. Huffman, Nature (London) **347**, 354 (1990).
[30] P. A. Heiney, J. E. Fischer, A. R. McGhie, W. J. Romanow, A. M. Denenstein, J. P. McCauley, Jr., Amos B. Smith, III, and D. E. Cox, Phys. Rev. Lett. **66**, 2911 (1991).
[31] P. D. Godwin, S. D. Kenny, and R. Smith, Surf. Sci. **529**, 237 (2003).